ACS APPLIED MATERIALS & INTERFACES

Research Article

Cite This: ACS Appl. Mater. Interfaces 2019, 11, 32826−32832

www.acsami.org

Suppressing Corrosion of Aluminum Foils via Highly Conductive Graphene-like Carbon Coating in High-Performance Lithium-Based Batteries

Xia Li,[†] Sixu Deng,[†] Mohammad Norouzi Banis,[†] Kieran Doyle-Davis,[†] Dongxing Zhang,[†] Tengyuan Zhang,[†] Jun Yang,[†] Ranjith Divigalpitiya,[‡] Frank Brandys,[‡] Ruying Li,[†] and Xueliang Sun*[,†]

[†]Department of Mechanical and Materials Engineering, University of Western Ontario, London, ON N6A 5B9, Canada

[‡]3M Canada Company, 1840 Oxford Street East, London, ON N5V 3R6, Canada

Supporting Information

ABSTRACT: Aluminum foil is the predominant cathodic current collector in lithium-based batteries due to the high electronic conductivity, stable chemical/electrochemical properties, low density, and low cost. However, with the development of next-generation lithium batteries, Al current collectors face new challenges, such as the requirement of increased chemical stability at high voltage, long-cycle-life batteries with different electrolyte systems, as well as improved electronic conductivity and adhesion for new electrode materials. In this study, we demonstrate a novel graphene-like carbon (GLC) coating on the Al foil in lithium-based batteries. Various physical and electrochemical characterizations are conducted to reveal the electronic conductivity and electrochemical stability of the GLC-Al foil in both carbonate- and ether-based electrolytes. Full-cell tests, including Li−S batteries and high-voltage Li-ion batteries, are performed to demonstrate the significantly improved cycling and rate performance of batteries with the use of the GLC-Al foil as current collectors. The cell using the GLC-Al foil can greatly reduce the potential polarization in Li−S batteries and can obtain a reversible capacity of 750 mAh g^{-1} over 100 cycles at 0.5C. Even with high-sulfur-loading cathodes, the Li−S battery at 1C still maintains over 500 mAh g^{-1} after 100 cycles. In high-voltage Li-ion batteries, the GLC-Al foil significantly improves the high-rate performance, showing an increased retained capacity by over 100 mAh g^{-1} after 450 cycles at 1C compared to the bare foil. It is believed that the developed GLC-Al foil brings new opportunities to enhance the battery life of lithium-based batteries.

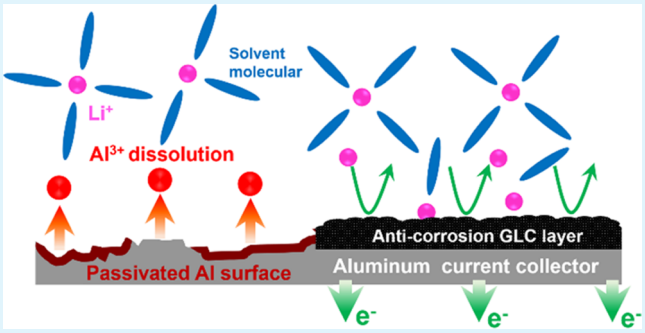

KEYWORDS: *aluminum foil, current collector, electrolytes, graphene-like carbon coating, electrochemical stability*

INTRODUCTION

Lithium (-ion) batteries are considered one of the most important energy storage devices for electric vehicles.[1−3] Current collectors, a critical component in batteries, directly determine the cycle life and performance of these cells.[4−6] An ideal current collector should first have enough electronic conductivity for the electrodes. Furthermore, the current collector should also have stable chemical and electrochemical properties to tolerate the various working environments of different battery systems.[4,6,7]

Al foil has been developed as the most predominant cathodic current collector in commercial Li (-ion) batteries due to the high electronic conductivity, low density, and affordable price.[8] However, with the development of next-generation batteries, Al foils face many challenges. First, the stability of Al foil in Li-ion electrolyte has been questioned. Some research reports that the naturally formed Al_2O_3 surface is not enough to resist corrosion from the electrolyte. Especially at high voltages over 3.0 V, the Li salts in the electrolyte, such as $LiPF_6$, $LiClO_4$, and LiTFSI, will attack and oxidize the Al foil into Al^{3+} ion dissolving into the electrolyte.[9,10] Especially of the high-voltage cathode materials in Li-ion batteries, such as spinel cathode $LiNi_{0.5}Mn_{1.5}O_4$ (LNMO) and Ni-rich cathode $LiNi_{1-x-y}Mn_xCo_yO_2$ (NMC), the high-working voltage leads to severe degradation of the current collector and undeniably shortens the cycling life of these batteries.[11,12] Second, the development of high-energy and high-loading cathodes, such as insulated sulfur cathodes in Li−S and Na−S batteries, brings new requirements of current collectors. Al foil should have strong surface interactions to bond nano-/microcathode particles without fracture or exfoliation of the electrode materials.[5−7] Furthermore, improved electronic conductivity is required to allow a sizeable current flow coming through high-loading cathodes.[5−7] Moreover, to realize high-energy batteries, the Al foils are also required to be thin, light, and possess enough mechanical

Received: April 12, 2019
Accepted: August 15, 2019
Published: August 15, 2019

DOI: 10.1021/acsami.9b06442
ACS Appl. Mater. Interfaces 2019, 11, 32826−32832

strength to reduce the weight of inert components in batteries. Many studies have been conducted in this field, including the development of the novel two-dimensional (2D)/three-dimensional (3D)-structured Al foils, the development of highly conductive coating materials for Al foils, and the development of metal oxide/sulfide/carbide/nitride catalysts on current collectors.[13−18]

In this study, we investigate a controllable graphene-like carbon (GLC) thin film as a coating material for Al foils in Li batteries to enhance the electronic conductivity and suppress the corrosion from the electrolyte. Various physical and electrochemical characterizations are described to demonstrate the anticorrosion effect of the coating layer for Al foil in both carbonate- and ether-based electrolytes. Full-battery tests of the as-prepared Al foils in Li−S and Li-ion batteries are also investigated. Our design of the GLC-coating layer for a highly stable and conductive Al foil as a current collector may bring new opportunities to further improve the battery life of Li (-ion) batteries.

RESULTS AND DISCUSSION

Physical characterizations of as-prepared Al foils are illustrated in Figure 1. Compared to the bare Al foil (Figure 1a), the Al foil with the GLC-coating layer demonstrates a dark metallic color in the visual image, and the SEM image presents a rough and uniform carbon coating on the surface (Figure 1b, left). From the enlarged SEM image (Figure 1b, low-right), the GLC-Al foil presents the irregularly layered structure graphene sheets covered on the surface. Raman spectroscopy is utilized to investigate the physical properties of the GLC-coating layer. As shown in Figure 1c, compared with the bare Al foil, the GLC-Al foil exhibits firm Raman peaks assigned to carbon in the spectrum. Notably, the appearance of the D′ peak and 2D peak in the spectrum demonstrates the graphene feature of the as-prepared carbon-coating layer.[19,20] Further, the peak intensity ratio of 2D to G peak illustrates that the GLC is composed of few-layer graphene.[21] It has been reported that the fewer the number of graphene layers, the better the conductivity of the material.[22,23] Surface roughness characterization is carried out via atomic force microscopy (AFM). As shown in Figure S1, the surface of the GLC-Al foil is significantly rougher than that of the bare foil; this is reflected in the measured average roughness (R_a) value of the two foils. As reported by the previous literature, the enhanced roughness of the current collector may improve the adhesion between electrode materials and current collector, which can facilitate the electrochemical performance of batteries.[24,25] Synchrotron-based X-ray absorption near-edge spectroscopy (XANES) is investigated to evaluate the property of Al foils before and after the coating process. As shown in Figure 1d, Al K-edge spectra of bare and coated Al foils are nearly identical, indicating that the GLC-coating synthetic process will not change the Al foil property. Based on the characterizations mentioned above, the as-prepared GLC-Al foil with few-layer graphene is well synthesized with high electronic conductivity for battery applications.

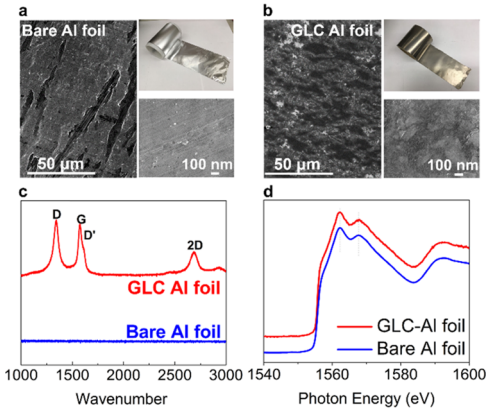

Figure 1. Physical characterizations of as-prepared Al foils. (a, b) field emission scanning electron microscope (FE-SEM) images and visual images, (c) Raman spectra, and (d) Al K-edge XANES spectra of bare and GLC-Al foils.

In addition to electronic conductivity, the anticorrosion of Al foil in an electrochemical environment is another indicator related to the performance of the current collector in batteries. To investigate the electrochemical properties of Al foils, Li−Al cells are fabricated in carbonate- and ether-based electrolytes. To ensure the consistency of the testing condition of lithium-based full cells, the voltage window in the carbonate electrolyte is in 1−5 V (for high-voltage Li-ion batteries), while it is 1−3.5 V in the ether-based electrolyte (for most Li−S batteries). As shown in the cyclic voltammograms (CVs) in Figure 2a,b, the

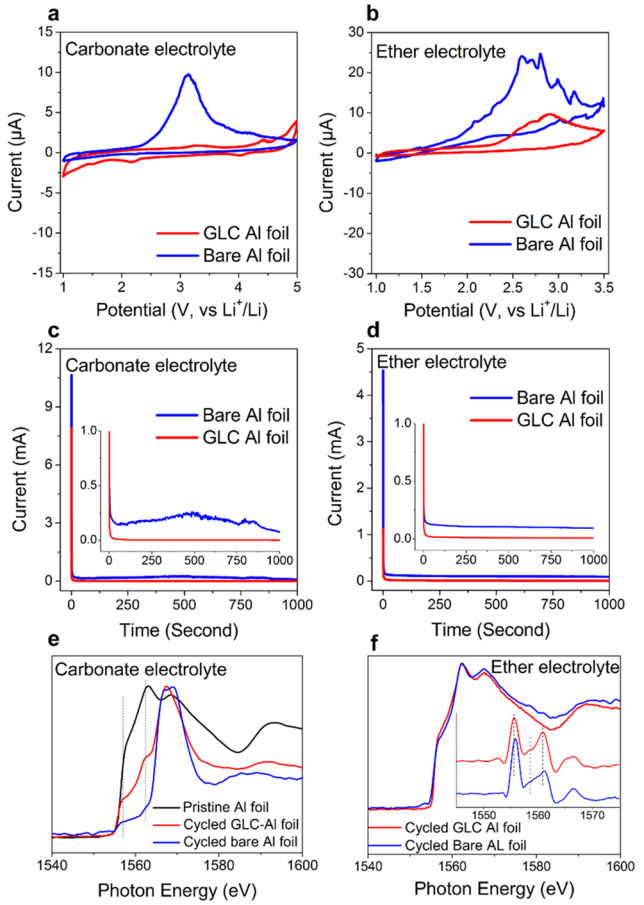

Figure 2. Electrochemical characterizations of Al foils. CV profiles of Li−Al cells in (a) the carbonate electrolyte and (b) the ether electrolyte. Chronoamperograms of Li−Al cells (c) at 4.5 V in the carbonate-based electrolyte and (d) at 3.0 V in the ether-based electrolyte; (e, f) Al K-edge XANES spectra of as-prepared Al foils cycled in Li−Al cells.

DOI: 10.1021/acsami.9b06442
ACS Appl. Mater. Interfaces 2019, 11, 32826−32832

bare Al foils in both carbonate and ether electrolytes demonstrate an apparent anodic peak with currents of over 9.7 μA (carbonate) and 24.5 μA (ether) at the first cycle, respectively. This result indicates that the bare Al foils are unstable at high voltage in the electrochemical operating window and that Al metal is attacked by the electrolyte and further oxidized to Al^{3+} in an anodic process.[8,9] The previous literature indicates that the anodic peaks are associated with the passivating process of the Al foil surface with the decomposition of Li salt.[26−29] On the other hand, GLC-Al foils in the two electrolytes show a much smaller current peak during the whole CV process, demonstrating the improved stability of Al foils with the GLC-coating layer. Chronoamperograms of the Al foils in carbonate and ether electrolytes are illustrated in Figure 2c,d. In the carbonate-based electrolyte, the polarization voltage of the cell is set at 4.5 V and held for 1 h. Interestingly, the current for the bare Al foil increased to over 10 mA sharply and gradually decreased to 250 μA in the following 1000 s. However, for the GLC-Al foil, the initial current maximum is much smaller (7.8 mA) and the current drops to a much lower stable steady-state current (1 μA) compared to the bare foil. In the ether-based electrolyte (Figure 2d), the same pattern persists, with a rapid drop in initial current maxima to a steady-state current, with GLC-Al being significantly lower than the bare foil. As reported by the previous literature, a higher current value indicates a more serious corroded process of the Al foil, and therefore the results agree with the CV curves that the GLC layer helps to suppress the corrosion of the Al foil with fewer side reactions during the electrochemical activity.[10,30] Al K-edge XANES spectra of Al foils after electrochemical testing were conducted to further investigate the chemical reaction occurring in the Al foils. As shown in Figure 2e, compared to the Al foil before the electrochemical test, both the bare and GLC-Al foils show noticeable changes after electrochemical testing in the carbonate electrolyte. A new peak at 1570 eV appears, which can be assigned to the formation of Al^{3+} such as AlF_3 at the surface.[31,32] Interestingly, the GLC-Al foil (red line) still maintains the features from the pristine Al foil (1557 and 1562.4 eV), while these peaks are nearly nonexistent in the bare Al foil (blue line). These results indicate that the GLC layer to some extent protects the Al foil from the attack of the electrolyte and subsequent oxidation to Al^{3+} ions in the electrolyte. Figure 2f presents the Al K-edge XANES of Al foils operated in the ether-based electrolyte. The Al K-edge spectra of Al foils in the ether-based electrolyte do not demonstrate a noticeable change as in the carbonate electrolyte. This may be due to the operating voltage window in the ether-based electrolyte (1.0−3.0 V), as it is much milder than in the carbonate electrolyte (1.0−5.0 V), which indicates that the high operating voltage brings more challenges to Al foils. Compared to the first derivative XANES inserted in Figure 2f, the white line of the bare Al foil after cycling presents a slight shift to a higher energy than that of the GLC-Al foil (1555.5−1555. 8 eV), indicating the mild oxidation of the Al foil without the protection of the GLC layer.[31−33]

Surface morphologies of Al foils after cycling in Li−Al cells with two electrolytes are illustrated in Figure 3. As shown in Figure 3a−c, the bare Al foil after cycling demonstrates severe corrosion on the surface with a corroded porous structure. For the GLC-Al foils, on the other hand, it still maintains the carbon coating on the surface without any trace of corrosion. After cycling in the carbonate electrolyte, the GLC-Al foil

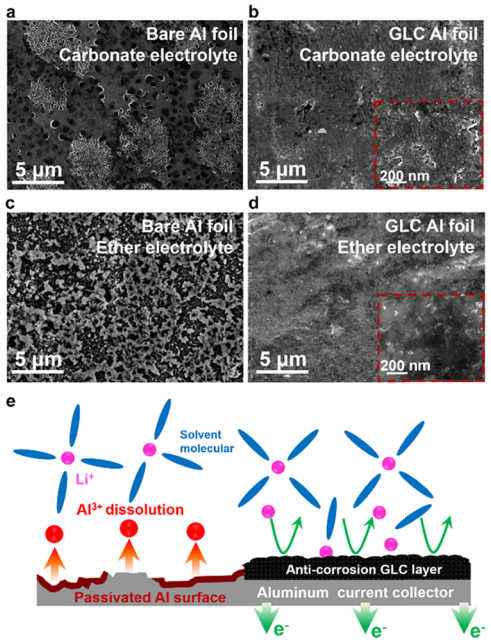

Figure 3. Morphology and schematic figures of Al foils after cycling. (a−d) SEM images of Al foils cycled 500 times in carbonate and ether electrolytes, respectively. (e) Schematic figure of the corrosion process of Al foils with and without GLC layer in Li-ion electrolytes.

(Figure 3b) is covered by a dense film on the surface, which may be related to the side reactions with the electrolyte at a high operating voltage and the solid electrolyte interphase layer formation at the cathode side. For the battery cycling in the ether electrolyte, carbon coating still remains on the surface of the GLC-Al foil (Figure 3d) and the morphologic feature of the graphene sheet in the enlarged image can be observed, which is close to the pristine GLC-Al foil shown in Figure 1. Based on the results obtained in Figures 2 and 3, a schematic illustration is presented in Figure 3e. The bare Al foil is very easily attacked by the electrolyte at high voltage and may be oxidized to Al^{3+} components, such as Al_2O_3 and AlF_3, or dissolved into the electrolyte. The corroded Al foil may weaken the connection between the electrode materials and current collector, which may worsen the electronic conductive network and deteriorate the battery performance.[34,35] Conversely, the GLC-coating layer acts as a corrosion inhibitor that protects the Al foil from these side reactions, which helps to maintain the integrity and electronic conductivity of the Al foil in the harsh electrochemical conditions of next-generation lithium batteries.

To further demonstrate the improved performance of GLC-Al foils, various full-cell configurations with the use of the two electrolyte systems were investigated. Electrochemical characterizations of sulfur cathodes with different Al foils in Li−S batteries are demonstrated in Figure 4. Detailed C−S composite preparation and physical characterizations are shown in the experimental section and Figure S2. As shown in Figure 4a, the sulfur cathode with the GLC-Al foil cycled at 800 mA g^{-1} presents a discharge capacity of over 1278 mAh g^{-1} and maintains 712 mAh g^{-1} after 100 cycles. However, the sulfur cathode with the bare Al foil at the same testing condition only maintains 475 mAh g^{-1} after 100 cycles. The cycling performance of the high-loading sulfur cathode (sulfur loading = 2 mg cm^{-2}) at 1C is shown in Figure S3. After 100 cycles, the discharge capacity is maintained over 500 mAh g^{-1},

DOI: 10.1021/acsami.9b06442
ACS Appl. Mater. Interfaces 2019, 11, 32826−32832

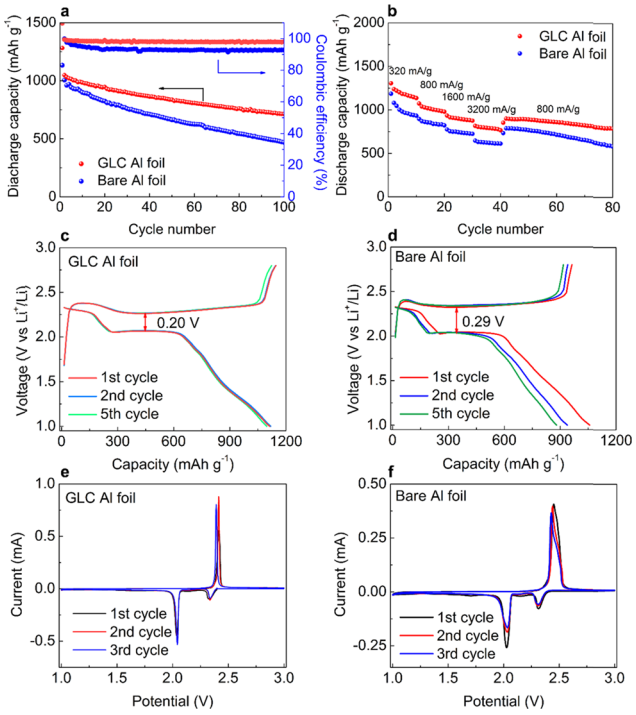

Figure 4. Electrochemical performance of sulfur cathodes with bare and GLC-Al foils as current collectors. (a) Discharge−charge cycling performance at 800 mA g^{-1}; (b) rate performance with various current densities; (c, d) discharge−charge profiles; and (e, f) CV curves of as-prepared Li−S batteries.

indicating good cycling performance of high-loading sulfur cathodes with the use of the GLC-AL foil as current collectors. The rate performance of the sulfur cathodes with the GLC-Al and bare Al foils is shown in Figure 4b. The sulfur cathode with the GLC-Al foil also demonstrates an improved performance at various current densities compared to that with the bare foil. The excellent cycling and rate performance of the sulfur cathodes with the GLC-Al foil illustrate the improved reaction reversibility and high conductivity of sulfur electrodes with the support of GLC-Al foils.[36−38] Figure 4c,d exhibits the discharge−charge curves of sulfur cathodes in different cycles. All of the sulfur cathodes present two potential plateaus at around 2.3 and 2.1 V, corresponding to the two-step reduction process where sulfur molecules are reduced to long-chain polysulfides and then to sulfides.[39−41] The sulfur cathodes with the GLC-Al foil demonstrate a smaller discharge−charge potential plateau gap (0.20 V) than those of the bare Al foil (0.29 V) during cycling, which indicates the smaller potential polarization of batteries with the GLC-Al foil. Corresponding dQ/dV plots are shown in Figure S4. The sulfur cathode with the GLC-Al foil demonstrates higher cathodic (2.069 V) and lower anodic potential features (2.266 V) compared with that of the bare Al foil, indicating the improved Li−S redox reaction kinetics and lower potential polarization of batteries with the support of the GLC-Al foil.[42] As shown in Figure 4e,f, the comparison of CV results also illustrates the improved electrochemical reaction activity of sulfur cathodes with the GLC-Al foil. The sulfur cathode with the GLC-Al foil presents sharper redox peaks with higher intensity compared to that of the bare foil. All of the electrochemical characterizations demonstrate the improved performance of Li−S cells with the use of the GLC-Al foil,

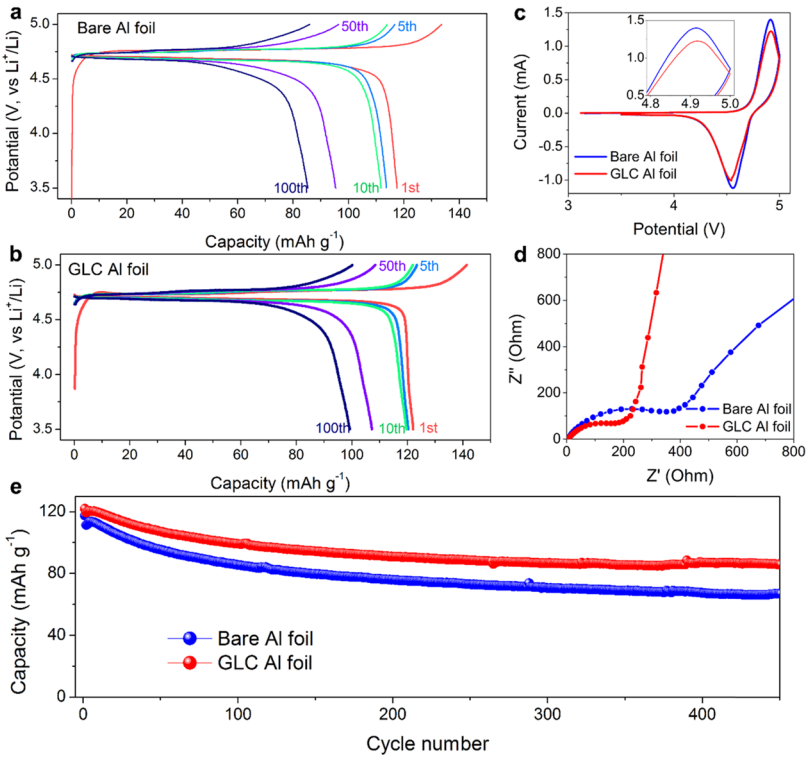

Figure 5. Electrochemical performance of as-prepared LNMO cathodes with bare and GLC-Al foils as current collectors. (a, b) Charge−discharge profiles, (c) CV profiles scanned at 0.5 mV s^{-1}, (d) EIS plots of the batteries after cycling, and (e) long-cycle performance of as-prepared batteries at 1C.

DOI: 10.1021/acsami.9b06442
ACS Appl. Mater. Interfaces 2019, 11, 32826−32832

which indicates that the GLC-coating layer helps sulfur cathodes with enhanced reaction reversibility during the electrochemical process. Electrochemical impedance spectroscopy (EIS) was also carried out, as shown in Figure S5. The spectra are composed of one semicircle and a straight line, which are corresponding to the surface charge transfer and Li-ion diffusion process.[36,37,43] With the GLC-Al foil as a cathodic current collector, the Li−S cell demonstrates a smaller surface charge-transfer resistance compared with the battery with the bare Al foil both before and after cycling test.

The thickness and aging factors of the GLC-coating layer are also investigated. As shown in Figure S6, the morphology of GLC-Al foils with different thicknesses and corresponding electrochemical performance are carried out. Interestingly, the cycling performances of sulfur cathodes with any thickness of GLC coatings are very similar. The thin and uniform coating is beneficial for the Al current collector to maintain its light specific mass in batteries.[5] To investigate the aging effect of the GLC-Al foil, physical and electrochemical characterizations of the GLC-Al foil produced 3 years ago was conducted, as shown in Figure S7. The 3 year GLC-Al foil demonstrates similar results in physical characterization and battery tests, indicating the excellent stability of the as-prepared GLC-Al foil for prolonged storage.

Spinel $LiNi_{0.5}Mn_{1.5}O_4$ (LNMO) cathode is employed to further investigate the current collector performance in the carbonate electrolyte at high voltage. LNMO is an attractive Li-ion cathode due to its high specific capacity and high-working voltage (4.7 V).[44] However, such high-working voltage leads to the decomposition of the electrolyte at the Al current collector surface.[45,46] Especially operating at high current density, such electrochemical environment may result in the rapid degradation of the Al foil current collector and fast decay of cycling capacity.[11,47,48] Figure 5a,b illustrates the discharge−charge profiles at 1C. Impressively, the potential polarization of batteries with the use of the GLC-Al foil is reduced than that of the bare Al foil. Furthermore, the capacity maintenance of the battery with the GLC-Al foil is also improved significantly compared to that with the bare one. The discharge capacity retains over 100 mAh g^{-1} of GLC-Al after 100 cycles, while the bare foil retains only 85 mAh g^{-1}. To further evaluate the potential polarization and resistance of batteries, CV and EIS tests are conducted. As shown in Figure 5c, the CV curve of the LNMO cathode at 5 V with the GLC-Al foil has a lower current than that with the bare Al one, indicating the reduced potential polarization of batteries at such high voltage. EIS plots of batteries after cycling are shown in Figure 5d. The diameter of the circle implies the surface charge-transfer resistance of batteries. After long-term cycling, the battery with the bare Al foil shows a much larger surface charge-transfer resistance than that with the GLC-Al foil. As shown by the electrochemical corrosion results in Figure 2, the bare Al foil after cycling in the carbonate electrolyte continuously breaks down and forms a lower conductivity-pitted Al surface, which will significantly increase the resistance at the interface between the electrode and current collector. Furthermore, as shown in the SEM images in Figure 3, the bare Al foil demonstrates a corroded surface structure after cycling in the carbonate electrolyte, weakening the adhesion between the active electrode materials and current collector, leading to an increased charge-transfer resistance in these cells. Figure 5e demonstrates the long-cycle performance of LNMO at 1C with the use of different Al foils as current collectors. Impressively, with the use of the GLC-Al foil, the capacity still maintains over 99 mAh g^{-1} over 450 cycles, which is over 1.5 times of the battery with the bare Al foil. The full-cell characterizations of Li-ion batteries further indicate that the GLC layer helps to protect the Al current collector at high voltage to maintain the electronic conductivity of electrodes and therefore minimize the battery resistance during cycling. As a result, the GLC-Al-foil-supported electrodes in Li-ion batteries offer improved high-rate performance with the prolonged cycling life. In the future, COMSOL simulation will be conducted and combined with the experimental result to further understand the electron transport process in the GLC-Al foil.[49−52]

CONCLUSIONS

In conclusion, we demonstrate a highly conductive and controllable graphene-like carbon coating for Al current collectors. The developed GLC-Al foil exhibits a much improved electrochemical stability in carbonate-based and ether-based electrolytes compared to the bare Al foil. Synchrotron-based XANES and other characterizations such as chronoamperometry indicate that the GLC layer protects the Al foil from electrolyte corrosion and effectively avoids the oxidation of the Al foil in an electrochemical environment. Furthermore, the Li−S and Li-ion battery characterizations demonstrate that the GLC-Al foil as a cathodic current collector is able to significantly improve the cycling stability and rate capacity. The cell using the GLC-Al foil can greatly reduce the potential polarization in Li−S batteries and can obtain a reversible capacity of 750 mAh g^{-1} over 100 cycles at 0.5C. In LNMO Li-ion batteries, the GLC-Al foil significantly increases the high-rate performance that the retained capacity is over 100 mAh g^{-1} after 450 cycles at 1C. Based on the obtained results, it is believed that the GLC coating for the Al foil would open up new opportunities to stabilize and optimize the performance of current collectors for next-generation Li batteries and the GLC carbon-coating method can be further applied to other 2D and 3D current collectors for batteries in the future.

EXPERIMENTAL SECTION

Preparation of Carbon−Sulfur Composites. KJ EC-600 carbon black powder was employed as a host for sulfur. For the C−S composite preparation, carbon black powder was first mixed with sulfur powder (99.5%, Sigma-Aldrich) for over 1 h by hand. The mixture was dried at 80 °C over 12 h and then transferred to a sealed reactor. During the two-step heating process, the C−S mixture was treated at 150 °C for 9 h and 300 °C for 2 h. The sulfur content of C−S composites was 68−70 wt %.

Preparation of Cathode Electrodes with Different Al Foils and Battery Assembly. The bare and GLC-Al foils are employed as cathodic current collectors. A detailed synthesis process of the GLC coating was reported in our previous studies and US patents.[53,54] The electrode slurry was composed of active material, acetylene black, and poly(vinylidene fluoride-*co*-hexafluoropropylene) (PVDF-HFP) in a ratio of 80:10:10. The slurry was cast on as-prepared Al foils and then dried at 60 °C under vacuum. For battery assembly, CR-2032-type coin cell is employed. A typical cell is composed of an as-prepared cathode electrode, a separator (Celgard 2400), and a Li foil. Carbonate-based electrolyte (1 M $LiPF_6$ in EC/DEC = 1:1, volume ratio) and ether-based electrolyte systems (1 M LiTFSI in dimethoxyethane/dioxolane 1:1, volume ratio) were selected for Li-ion and Li−S batteries in this research, respectively. Each cell contains 150 μL of the electrolyte.

DOI: 10.1021/acsami.9b06442
ACS Appl. Mater. Interfaces 2019, 11, 32826−32832

Electrochemical Characterization. All of the CV, EIS, and polarization tests were conducted on a potentiostation 3/Z (VMP3). For Li/Al cells, CV profiles were collected at 0.1 mV s^{-1} between 1.0 and 3.5 V when using the ether-based electrolyte and 1.0 and 5.0 V when using the carbonate-based electrolyte. In chronoamperometry characterization, cells were first charged to designate voltage (3.0 V in the ether-based electrolyte and 4.5 V in the carbonate electrolyte) with a linear scan of 10 mV s^{-1} and then maintain at the voltage to record the value evolution of the current. For Li−S batteries, CV profiles were collected at 0.1 mV s^{-1} between 1.0 and 3.0 V. For Li-ion batteries, CV profiles were collected at 0.5 mV s^{-1} between 3.0 and 5.0 V. EIS was performed with a 5 mV amplitude from 100 to 100 mHz. Li-ion and Li−S battery charge−discharge cycling tests were measured using a Landlike electrochemical station. The cutoff voltage of Li−S batteries was 1.0−3.0 V and of Li-ion batteries was 3.5−5.0 V.

Physical Characterization. The morphologies of Al foils and C−S electrodes were carried out by a Hitachi S-4800 field emission scanning electron microscope (FE-SEM). Thermogravimetric analysis (TGA) was measured on an SDT Q600 (TA Instruments) in N_2 atmosphere to determine the sulfur content of C−S composites. Raman scattering spectra were carried out by a HORIBA Scientific LabRAM HR Raman spectrometer system (532.4 nm). Surface roughness characterization is conducted via a Nanoscope V atomic force microscopy (Veeco, Inc.). Synchrotron-based X-ray absorption near-edge structure (XANES) was carried out at the Canadian Light Source (CLS). Al K-edge XANES was measured in total electron yield mode on the high-resolution spherical grating monochromator (SGM) beamline. For sample preparation, the Al foils after electrochemical testing were collected by opening the coin cells in an argon-filled glovebox. The cycled Al foils were then quickly transferred to the SGM beamlines for XANES characterization.

■ ASSOCIATED CONTENT

Supporting Information

The Supporting Information is available free of charge on the ACS Publications website at DOI: 10.1021/acsami.9b06442.

AFM images of bare and GLC-coated Al foil; FE-SEM image and TGA curve of as-prepared carbon−sulfur composites; cycling performance of the sulfur cathodes with different sulfur loadings at various current densities; dQ/dV plots of as-prepared Li−S batteries in different discharge−charge cycles; EIS spectra of as-prepared Li−S batteries with different current collectors; FE-SEM images in cross-sectional view of GLC-Al foils and cycle performance; Raman spectra and electrochemical characterizations of a 3 year GLC-Al foil (PDF)

■ AUTHOR INFORMATION

Corresponding Author

*E-mail: xsun@eng.uwo.ca.

ORCID

Mohammad Norouzi Banis: 0000-0002-6144-6837

Xueliang Sun: 0000-0003-2881-8237

Notes

The authors declare the following competing financial interest(s): Ranjith Divigalpitiya and Frank Brandys are employed by 3M Canada Company.

■ ACKNOWLEDGMENTS

This research was supported by the 3M Canada, Natural Science and Engineering Research Council of Canada (NSERC), Canada Research Chair Program (CRC), Canada Foundation for Innovation (CFI), Canada Light Source at University of Saskatchewan (CLS), and Western University (UWO). X.L. thanks the funding support of Mitacs Elevate Postdoctoral Fellowship.

■ REFERENCES

(1) Ji, X.; Nazar, L. F. Advances in Li-S Batteries. *J. Mater. Chem.* **2010**, *20*, 9821−9826.

(2) Bruce, P. G.; Freunberger, S. A.; Hardwick, L. J.; Tarascon, J. M. Li-O_2 and Li-S Batteries with High Energy Storage. *Nat. Mater.* **2012**, *11*, 19−29.

(3) Goodenough, J. B.; Park, K. S. The Li-ion Rechargeable Battery: A Perspective. *J. Am. Chem. Soc.* **2013**, *135*, 1167−1176.

(4) Rodrigues, M.-T. F.; Babu, G.; Gullapalli, H.; Kalaga, K.; Sayed, F. N.; Kato, K.; Joyner, J.; Ajayan, P. M. A Materials Perspective on Li-Ion Batteries at Extreme Temperatures. *Nat. Energy* **2017**, *2*, No. 17108.

(5) Yang, X.; Li, X.; Adair, K.; Zhang, H.; Sun, X. Structural Design of Lithium−Sulfur Batteries: From Fundamental Research to Practical Application. *Electrochem. Energy Rev.* **2018**, *1*, 239−293.

(6) Li, X.; Sun, X. Interface Design and Development of Coating Materials in Lithium-Sulfur Batteries. *Adv. Funct. Mater.* **2018**, *28*, No. 1801323.

(7) Peng, H.-J.; Huang, J.-Q.; Cheng, X.-B.; Zhang, Q. Review on High-Loading and High-Energy Lithium-Sulfur Batteries. *Adv. Energy Mater.* **2017**, *7*, No. 1700260.

(8) Zhang, S. S.; Jow, T. R. Aluminum Corrosion in Electrolyte of Li-Ion Battery. *J. Power Sources* **2002**, *109*, 458−464.

(9) Peng, C.; Yang, L.; Zhang, Z.; Tachibana, K.; Yang, Y.; Zhao, S. Investigation of the Anodic Behavior of Al Current Collector in Room Temperature Ionic Liquid Electrolytes. *Electrochim. Acta* **2008**, *53*, 4764−4772.

(10) Kramer, E.; Passerini, S.; Winter, M. Dependency of Aluminum Collector Corrosion in Lithium Ion Batteries on the Electrolyte Solvent. *ECS Electrochem. Lett.* **2012**, *1*, C9−C11.

(11) Suo, L.; Xue, W.; Gobet, M.; Greenbaum, S. G.; Wang, C.; Chen, Y.; Yang, W.; Li, Y.; Li, J. Fluorine-Donating Electrolytes Enable Highly Reversible 5-V-Class Li Metal Batteries. *Proc. Natl. Acad. Sci. U.S.A.* **2018**, *115*, 1156−1161.

(12) Xiao, B.; Sun, X. Surface and Subsurface Reactions of Lithium Transition Metal Oxide Cathode Materials: An Overview of the Fundamental Origins and Remedying Approaches. *Adv. Energy Mater.* **2018**, *8*, No. 1802057.

(13) Chung, S.-H.; Manthiram, A. Lithium-Sulfur Batteries with Superior Cycle Stability by Employing Porous Current Collectors. *Electrochim. Acta* **2013**, *107*, 569−576.

(14) Kim, H.; Lee, J. T.; Yushin, G. High Temperature Stabilization of Lithium-Sulfur Cells with Carbon Nanotube Current Collector. *J. Power Sources* **2013**, *226*, 256−265.

(15) Sun, L.; Kong, W.; Li, M.; Wu, H.; Jiang, K.; Li, Q.; Zhang, Y.; Wang, J.; Fan, S. Cross-Stacked Carbon Nanotube Film as An Additional Built-in Current Collector and Asorption Layer for High-Performance Lithium Sulfur Batteries. *Nanotechnology* **2016**, *27*, No. 075401.

(16) Liu, S.; Tang, S.; Zhang, X.; Wang, A.; Yang, Q. H.; Luo, J. Porous Al Current Collector for Dendrite-Free Na Metal Anodes. *Nano Lett.* **2017**, *17*, 5862−5868.

(17) Jin, S.; Jiang, Y.; Ji, H.; Yu, Y. Advanced 3D Current Collectors for Lithium-Based Batteries. *Adv. Mater.* **2018**, *30*, No. 1802014.

(18) Yun, Q.; He, Y. B.; Lv, W.; Zhao, Y.; Li, B.; Kang, F.; Yang, Q. H. Chemical Dealloying Derived 3D Porous Current Collector for Li Metal Anodes. *Adv. Mater.* **2016**, *28*, 6932−6939.

(19) Dillon, R.; Woollam, J.; Katkanant, V. Use of Raman Scattering to Investigate Disorder and Crystallite Formation in As-Deposited and Annealed Carbon Films. *Phys. Rev. B* **1984**, *29*, 3482−3489.

(20) Sadezky, A.; Muckenhuber, H.; Grothe, H.; Niessner, R.; Pöschl, U. Raman Microspectroscopy of Soot and Related Carbonaceous Materials: Spectral Analysis and Structural Information. *Carbon* **2005**, *43*, 1731−1742.

(21) Jaouen, F.; Serventi, A. M.; Lefèvre, M.; Dodelet, J.-P.; Bertrand, P. Non-Noble Electrocatalysts for O_2 Reduction: How Does

Heat Treatment Affect Their Activity and Structure? Part II. Structural Changes Observed by Electron Microscopy, Raman, and Mass Spectroscopy. *J. Phys. Chem. C* **2007**, *111*, 5971−5976.
(22) Geng, D.; Yang, S.; Zhang, Y.; Yang, J.; Liu, J.; Li, R.; Sham, T.-K.; Sun, X.; Ye, S.; Knights, S. Nitrogen Doping Effects on the Structure of Graphene. *Appl. Surf. Sci.* **2011**, *257*, 9193−9198.
(23) Sharifi, T.; Nitze, F.; Barzegar, H. R.; Tai, C.-W.; Mazurkiewicz, M.; Malolepszy, A.; Stobinski, L.; Wågberg, T. Nitrogen Doped Multi Walled Carbon Nanotubes Produced by CVD-Correlating XPS and Raman Spectroscopy for the Study of Nitrogen Inclusion. *Carbon* **2012**, *50*, 3535−3541.
(24) Jeon, H.; Cho, I.; Jo, H.; Kim, K.; Ryou, M.-H.; Lee, Y. M. Highly Rough Copper Current Collector: Improving Adhesion Property Between A Silicon Electrode and Current Collector for Flexible Lithium-Ion Batteries. *RSC Adv.* **2017**, *7*, 35681−35686.
(25) Yang, X.; Chen, Y.; Wang, M.; Zhang, H.; Li, X.; Zhang, H. Phase Inversion: A Universal Method to Create High-Performance Porous Electrodes for Nanoparticle-Based Energy Storage Devices. *Adv. Funct. Mater.* **2016**, *26*, 8427−8434.
(26) Zhang, X.; Devine, T. M. Factors That Influence Formation of AlF_3 Passive Film on Aluminum in Li-Ion Battery Electrolytes with $LiPF_6$. *J. Electrochem. Soc.* **2006**, *153*, B375−B383.
(27) Dahbi, M.; Ghamouss, F.; Tran-Van, F.; Lemordant, D.; Anouti, M. Comparative Study of EC/DMC LiTFSI and $LiPF_6$ Electrolytes for Electrochemical Storage. *J. Power Sources* **2011**, *196*, 9743−9750.
(28) Dahbi, M.; Ghamouss, F.; Tran-Van, F.; Lemordant, D.; Anouti, M. Ester Based Electrolyte with Lithium Bis(trifluoromethane sulfonyl) Imide Salt for Electrochemical Storage Devices: Physicochemical and Electrochemical Characterization. *Electrochim. Acta* **2012**, *86*, 287−293.
(29) Dahbi, M.; Komaba, S. Fluorine Chemistry for Negative Electrode in Sodium and Lithium Ion Batteries. *Adv. Fluoride-Mater. Energy Convers.* **2015**, 387−414.
(30) Richard Prabakar, S. J.; Hwang, Y.-H.; Bae, E. G.; Lee, D. K.; Pyo, M. Graphene Oxide as A Corrosion Inhibitor for the Aluminum Current Collector in Lithium Ion Batteries. *Carbon* **2013**, *52*, 128−136.
(31) Eltanany, G. Sol-Gel Synthesis and Properties of Nanoscopic Aluminum Fluoride. Humboldt-Universität zu Berlin, Mathematisch-Naturwissenschaftliche Fakultät I, 2007.
(32) Weiher, N.; Makarowicz, A.; Beesley, A. M.; Kemnitz, E.; Schroeder, S. L. M. Structure-Property Relationships in Solid AlF_3 Lewis Acids. *AIP Conf. Proc.* **2007**, *882*, 827−829.
(33) Neuville, D. R.; Cormier, L.; Roux, J.; Henderson, G. S.; de Ligny, D.; Flank, A.-M.; Lagarde, P. Investigation of Aluminate and Al_2O_3 Crystals and Melts at High Temperature Using XANES Spectroscopy. *AIP Conf. Proc.* **2007**, *882*, 419−421.
(34) Streipert, B.; Röser, S.; Kasnatscheew, J.; Janßen, P.; Cao, X.; Wagner, R.; Cekic-Laskovic, I.; Winter, M. Influence of $LiPF_6$ on the Aluminum Current Collector Dissolution in High Voltage Lithium Ion Batteries after Long-Term Charge/Discharge Experiments. *J. Electrochem. Soc.* **2017**, *164*, A1474−A1479.
(35) Theivaprakasam, S.; Girard, G.; Howlett, P.; Forsyth, M.; Mitra, S.; MacFarlane, D. Passivation Behaviour of Aluminium Current Collector in Ionic Liquid Alkyl Carbonate (Hybrid) Electrolytes. *npj Mater. Degrad.* **2018**, *2*, No. 13.
(36) Yuan, Z.; Peng, H.-J.; Huang, J.-Q.; Liu, X.-Y.; Wang, D.-W.; Cheng, X.-B.; Zhang, Q. Hierarchical Free-Standing Carbon-Nanotube Paper Electrodes with Ultrahigh Sulfur-Loading for Lithium-Sulfur Batteries. *Adv. Funct. Mater.* **2014**, *24*, 6105−6112.
(37) Zhou, G.; Paek, E.; Hwang, G. S.; Manthiram, A. Long-Life Li/Polysulphide Batteries with High Sulphur Loading Enabled by Lightweight Three-Dimensional Nitrogen/Sulphur-Codoped Graphene Sponge. *Nat. Commun.* **2015**, *6*, No. 7760.
(38) Li, X.; Banis, M.; Lushington, A.; Yang, X.; Sun, Q.; Zhao, Y.; Liu, C.; Li, Q.; Wang, B.; Xiao, W.; Wang, C.; Li, M.; Liang, J.; Li, R.; Hu, Y.; Goncharova, L.; Zhang, H.; Sham, T. K.; Sun, X. A High-Energy Sulfur Cathode in Carbonate Electrolyte by Eliminating Polysulfides via Solid-Phase Lithium-Sulfur Transformation. *Nat. Commun.* **2018**, *9*, No. 4509.
(39) Lu, S.; Cheng, Y.; Wu, X.; Liu, J. Significantly Improved Long-Cycle Stability in High-Rate Li-S Batteries Enabled by Coaxial Graphene Wrapping over Sulfur-Coated Carbon Nanofibers. *Nano Lett.* **2013**, *13*, 2485−2489.
(40) Li, X.; Li, X.; Banis, M. N.; Wang, B.; Lushington, A.; Cui, X.; Li, R.; Sham, T.-K.; Sun, X. A. Tailoring Interactions of Carbon and Sulfur in Li-S battery Cathode: Significant Effects of Carbon-heteroatom Bonds. *J. Mater. Chem. A* **2014**, *2*, 12866−12872.
(41) Rong, J.; Ge, M.; Fang, X.; Zhou, C. Solution Ionic Strength Engineering as a Generic Strategy to Coat Graphene Oxide (GO) on Various Functional Particles and Its Application in High-Performance Lithium-Sulfur (Li-S) Batteries. *Nano Lett.* **2014**, *14*, 473−479.
(42) Li, N.; Zheng, M.; Lu, H.; Hu, Z.; Shen, C.; Chang, X.; Ji, G.; Cao, J.; Shi, Y. High-Rate Lithium-Sulfur Batteries Promoted by Reduced Graphene Oxide Coating. *Chem. Commun.* **2012**, *48*, 4106−4108.
(43) Li, G.-C.; Li, G.-R.; Ye, S.-H.; Gao, X.-P. A Polyaniline-Coated Sulfur/Carbon Composite with an Enhanced High-Rate Capability as a Cathode Material for Lithium/Sulfur Batteries. *Adv. Energy Mater.* **2012**, *2*, 1238−1245.
(44) Deng, S.; Xiao, B.; Wang, B.; Li, X.; Kaliyappan, K.; Zhao, Y.; Lushington, A.; Li, R.; Sham, T.-K.; Wang, H.; Sun, X. New Insight into Atomic-Scale Engineering of Electrode Surface for Long-Life and Safe High Voltage Lithium Ion Cathodes. *Nano Energy* **2017**, *38*, 19−27.
(45) Ma, T.; Xu, G. L.; Li, Y.; Wang, L.; He, X.; Zheng, J.; Liu, J.; Engelhard, M. H.; Zapol, P.; Curtiss, L. A.; Jorne, J.; Amine, K.; Chen, Z. Revisiting the Corrosion of the Aluminum Current Collector in Lithium-Ion Batteries. *J. Phys. Chem. Lett.* **2017**, *8*, 1072−1077.
(46) Sayed, F. N.; Rodrigues, M. F.; Kalaga, K.; Gullapalli, H.; Ajayan, P. M. Curious Case of Positive Current Collectors: Corrosion and Passivation at High Temperature. *ACS Appl. Mater. Interfaces* **2017**, *9*, 43623−43631.
(47) Xiao, B.; Liu, H.; Liu, J.; Sun, Q.; Wang, B.; Kaliyappan, K.; Zhao, Y.; Banis, M. N.; Liu, Y.; Li, R.; Sham, T. K.; Botton, G. A.; Cai, M.; Sun, X. Nanoscale Manipulation of Spinel Lithium Nickel Manganese Oxide Surface by Multisite Ti Occupation as High-Performance Cathode. *Adv. Mater.* **2017**, *29*, No. 1703764.
(48) Liu, W.; Li, X.; Xiong, D.; Hao, Y.; Li, J.; Kou, H.; Yan, B.; Li, D.; Lu, S.; Koo, A.; Adair, K.; Sun, X. Significantly Improving Cycling Performance of Cathodes in Lithium Ion Batteries: The Effect of Al_2O_3 and $LiAlO_2$ Coatings on $LiNi_{0.6}Co_{0.2}Mn_{0.2}O_2$. *Nano Energy* **2018**, *44*, 111−120.
(49) Chen, Z.; Hsu, P.-C.; Lopez, J.; Li, Y.; To, J. W. F.; Liu, N.; Wang, C.; Andrews, Sean C.; Liu, J.; Cui, Y.; Bao, Z. Fast and Reversible Thermoresponsive Polymer Switching Materials for Safer Batteries. *Nat. Energy* **2016**, *1*, No. 15009.
(50) Zadin, V.; Brandell, D.; Kasemägi, H.; Aabloo, A.; Thomas, J. O. Finite Element Modelling of Ion Transport in the Electrolyte of a 3D-Microbattery. *Solid State Ionics* **2011**, *192*, 279−283.
(51) Appiah, W. A.; Park, J.; Van Khue, L.; Lee, Y.; Choi, J.; Ryou, M.-H.; Lee, Y. M. Comparative Study on Experiments and Simulation of Blended Cathode Active Materials for Lithium Ion Batteries. *Electrochim. Acta* **2016**, *187*, 422−432.
(52) Wang, S. H.; Yin, Y. X.; Zuo, T. T.; Dong, W.; Li, J. Y.; Shi, J. L.; Zhang, C. H.; Li, N. W.; Li, C. J.; Guo, Y. G. Stable Li Metal Anodes via Regulating Lithium Plating/Stripping in Vertically Aligned Microchannels. *Adv. Mater.* **2017**, *29*, No. 1703729.
(53) Divigalpitiya, R.; Buckett, M. Electrode Including Current Collector with Nano-Scale Coating and Method of Making the Same. U.S. Patent US9172085 B2, 2015.
(54) Divigalpitiya, R.; Ezugwu, S.; Fanchini, G. Carbon Coated Articles and Methods for Making the Same. U.S. Patent US10041748 B2, 2018.

DOI: 10.1021/acsami.9b06442
ACS Appl. Mater. Interfaces 2019, 11, 32826−32832